

AVERAGE FEATURES OF THE MUON COMPONENT OF EAS $\geq 10^{17}$ eV

P. R. BLAKE, M. LUKSYS, W. F. NASH and A. J. SEPHTON
University of Nottingham, England.

1. Method Three 10 m² liquid scintillators were situated at approximately 0 m, 150 m and 250 m from the centre of the Haverah Park array. The detectors were shielded by lead/barytes giving muon detection thresholds of 317 MeV, 431 MeV and 488 MeV respectively. During part of the operational period the 431 MeV threshold was lowered to 313 MeV for comparison purposes. For risetime measurement fast phototubes were used and the 10% to 70% amplitude time interval was parameterised by T_{70} .

2. The Muon Density Lateral Distribution A muon lateral density distribution of the form $\rho_{\mu}(R, \theta) = k[\rho(500)]^{0.94} 1/R(1 + R/490)^{-\eta}$ has been fitted to the data for $120 \text{ m} < R < 600 \text{ m}$ and $0.27 < \rho(500) < 2.55$. The shower 'size' parameter $\rho(500)$ is the water Cerenkov response at 500 m from the core of the EAS and is relatable to the primary energy (eg Hillas model A gives $E_p = 3.87 \times 10^{17} [\rho(500)]^{1.018}$). Table 1 shows the best fit values of k and η to the data for near vertical EAS. The results show general consistency.

SEC θ RANGE	DETECTOR			UNCERTAINTY		
	THRESHOLD MeV	NO. OF EAS	BEST FIT k	UNCERTAINTY IN k	BEST FIT η	UNCERTAINTY IN η
1.0-1.1	313	320	2060	± 150	2.77	± 0.15
	317	1056	2000	± 90	2.69	± 0.09
	431	925	1980	± 80	2.96	± 0.09
	488	803	1890	± 90	3.11	± 0.10

Table 1 Best fit values of k and η in the muon density lateral distribution.

Table 2 compares the values of muon density derived at 100 m core distance intervals from the Nottingham detectors for $\rho(500) = 1.15$. Also labelled are the data from other arrays where the intercalibration has been carried out on the basis of flux rates [Blake et al (1975) and (1981)]. The Akeno data is taken from Nagano et al (1984).

CORE DIST (m)	SYDNEY							
	NOTTM SCINT	NOTTM SCINT	NOTTM SCINT	NOTTM SCINT	SPARK CHAMB	GREISEN (1960)	YAKUTSK SCINT	AKENO PROP
	S-L 313MeV	S-L 317MeV	S-L 431MeV	S-L 488MeV	S-L 700MeV	S-L 1GeV	S-L 1GeV	930gcm ⁻² 1GeV
100	14.00	13.80	13.00	12.10	-	6.60	6.90	8.50
200	4.55	4.54	4.10	3.72	2.86	2.29	2.20	2.82
300	2.09	2.10	1.83	1.63	1.35	1.09	0.96	1.28
400	1.12	1.14	0.96	0.84	0.72	0.60	0.52	0.70
500	0.67	0.69	0.56	0.48	0.42	0.37	0.30	0.42
600	0.43	0.44	0.35	0.30	0.26	0.24	0.20	0.27

Table 2 Comparison of muon density lateral distribution (Muons m^{-2} for $\theta < 25^\circ$ and $E_p \sim 3.87 \times 10^{17}$ eV). [S-L = sea level]

Allowing for the different thresholds and altitudes the results show reasonably consistent agreement. Figure 1 plots the muon density data at 300 m as a function of threshold energy.

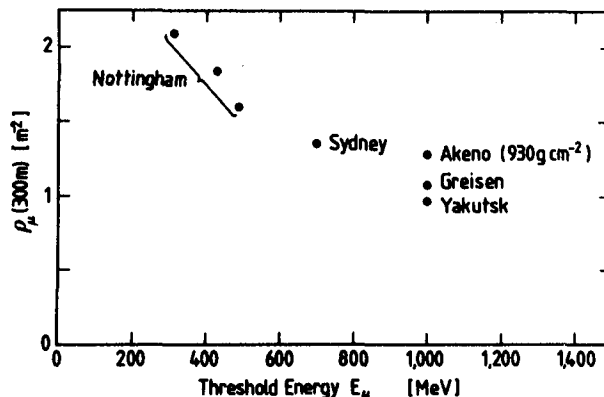


Figure 1 Muon density at 300 m as function of threshold energy.

The errors on individual points are estimated as $\sim 10\%$ and arise mainly from the intercalibration procedure.

Most nuclear cascade models yield distributions in agreement with the experimentally derived lateral distributions as regards slope.

Clearly absolute muon density predictions depend on both the primary mass composition assumed as well as the details of the cascade model.

3. Muon-water Cerenkov Ratio Figure 2 displays the muon-water Cerenkov density ratio as a function of R and θ for $\rho(500) = 1.15$ and $E_\mu = 317$ MeV. Again, on the whole, models predict the observed shape of the observed lateral distribution with reasonable closeness. However whilst Hillas (1971) model A fits the absolute value of the ratio well with a 100% proton primary beam; the Gaisser et al (1978) predictions require $A \sim 56$ to be compatible.

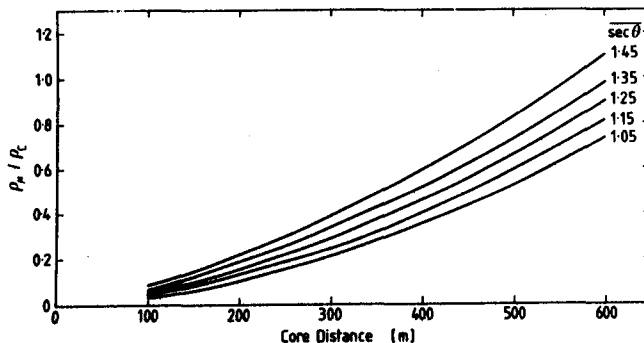


Figure 2 Muon-water Cerenkov density ratio (ρ_μ/ρ_c) as a function of core distance and $\sec\theta$.

4. The Average Time Spread (\bar{T}_0) Fast phototubes and electronics enable the time spread of the muons ($T_{70} = 10\%$ to 70% full amplitude) to be determined including an instrumental response $T_{70}=32$ ns.

Table 3 lists the derived values for T_{70} as a function of R for three of the threshold energies.

$R(m)$	313 MeV	431 MeV	488 MeV
200	57.9 ns	54.2 ns	53.4 ns
250	64.4 ns	59.2 ns	59.4 ns
300	70.9 ns	64.2 ns	65.4 ns
350	77.4 ns	69.2 ns	71.4 ns
400	83.9 ns	74.2 ns	77.4 ns
450	90.4 ns	79.2 ns	83.4 ns
500	96.9 ns	84.2 ns	89.4 ns

Table 3 Derived values of T_{70} for $\rho(500) = 1$ and $\sec\theta = 1$.

Figures 3 and 4 compare the experimentally derived data for T_{70} (at 431 MeV threshold) with the cascade calculations of McComb and Turver (1981). Clearly the experimental data are faster than the predictions even assuming a 100% iron primary flux.

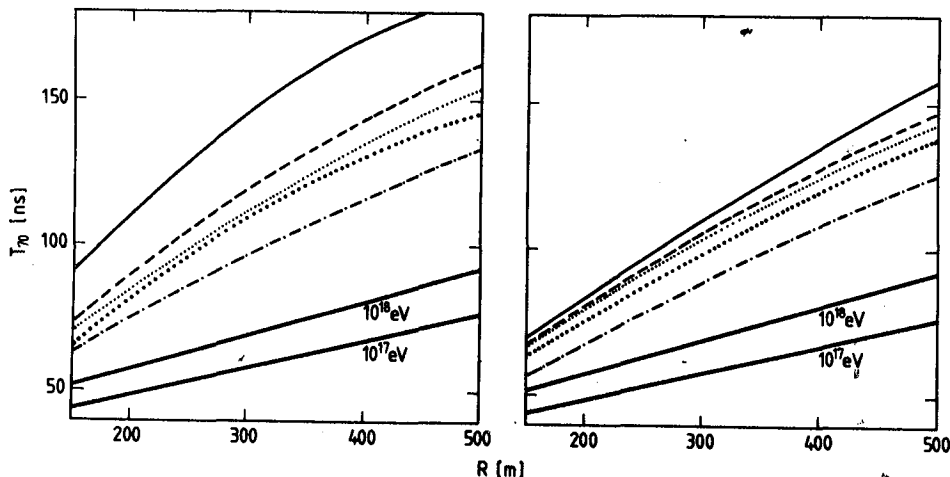


Figure 3 & 4 Comparison of predictions and experimental measurements of T_{70} as a function of R .
 — Experimental data best fits. McComb and Turver (1981)
 — simulations with
 — scaling, $\sigma = \text{const}$ - - - - - Landau, $E^{1/4}$, $\sigma = \text{const}$
 Landau, $E^{1/3}$, $\sigma = \text{const}$ Scaling, $\sigma = \ln^2 s$
 - . - . - Landau, $E^{1/3}$, $\sigma = \ln^2 s$ Fig. 3 Proton Fig. 4 Iron primaries

5. Elongation Length Both of the two parameters (μ/c and T_{70}) can be used to determine the 'elongation rate' of the EAS. The technique used has been described elsewhere (Blake et al, 1983). Calculations based on the data presented in this paper lead to an

elongation rate = $66(\pm 10) \text{ g cm}^{-2} \text{ decade}^{-1}$ from (μ/c) and $73(\pm 23) \text{ g cm}^{-2} \text{ decade}^{-1}$ from T_{70} . These results are in substantial agreement with other experimental data in the same energy range.

6. Conclusions The average lateral distribution of both the density and time spread of muons in EAS have been measured. The density measurements fit in well with those from other arrays and thus serve successfully for cross-checking of array calibrations.

The fast average risetime of the muons indicates early EAS development and little contribution from photoproduced muons at these primary energies.

Both the muon density and muon time spread are sensitive to small changes in threshold detection energy (both $\sim 6\%$ per 100 MeV at ~ 400 MeV threshold). Both measurements yield 'elongation rates' ($\sim 70 \text{ g cm}^{-2} \text{ decade}^{-1}$) in close agreement with other work.

These results support the general conclusion that the primary beam contains a significant proportion of light elements at these energies.

REFERENCES

- BLAKE, P. R., NASH, W. F., PRESCOTT, I. C. and STRUTT, R. B., 14th Int. Cosmic Ray Conf. Munich, 8, (1975).
- BLAKE, P. R., NASH, W. F., O'CONNELL, B., and STRUTT, R. B., 17th Int. Cosmic Ray Conf. Paris, 6, 8, (1981).
- GAISSER, T. K., PROTHEROE, R. J., TURVER, K. E. and McCOMB, T. J. L. Rev. Mod. Phys. 50 no.4 859 (1978).
- HILLAS et al. Proc. Int. Cos. Ray Conf., Hobart, 3, 1007 (1971).
- McCOMB, T. J. L. and TURVER, K. E., private communication (1981).
- NAGANO, M. et al. J. Phys. G 10, 1295 (1984).